SAND2020-0925C

Near-Zero Power Mechanical Shock-Resistant Inertial Wakeup System with Scaled Inputs

Sean Yen
Sandia National Laboratories
Albuquerque, USA
syen@sandia.gov

Benjamin A. Griffin
Microsystems Technology Office
Defense Advanced Research Projects Agency
Arlington, USA

Bryson Barney
ON Semiconductor
Lindon, USA
bryson.barney@onsemi.com

Adam M. Edstrand
Sandia National Laboratories
Albuquerque, USA
aedstra@sandia.gov

Andrew I. Young
Sandia National Laboratories
Albuquerque, USA
aiyoung@sandia.gov

Tammy Pluym
Sandia National Laboratories
Albuquerque, USA

Emily Donahue
Sandia National Laboratories
Albuquerque, USA
eadonah@sandia.gov

Robert W. Reger
Sandia National Laboratories
Albuquerque, USA
rwreger@sandia.gov

***Abstract*— This paper reports on a near-zero power inertial wakeup sensor system supporting digital weighting of inputs and with protection against false positives due to mechanical shocks. This improves upon existing work by combining the selectivity and sensitivity (*Q*-amplification) of resonant MEMS sensors with the flexibility of digital signal processing while consuming below 10 nW. The target application is unattended sensors for perimeter sensing and machinery health monitoring where extended battery life afforded by the low power consumption eliminates the need for power cables. For machinery health monitoring, the signals of interest are stationary but may contain spurious mechanical shocks.**

Keywords—inertial sensing, near-zero power sensing, unattended sensing

I. Introduction

Unattended, persistent sensing of infrequent events requires the minimization of sensor power consumption to prolong battery life [1]. Examples of applications include perimeter sensing and machinery health monitoring, which are hostile to the wiring of power cables and to the replacement of batteries. In a typical system, a near-zero power wakeup sensor would perform initial detection to wake up higher-powered sensors or a communications system to send an alert.

In this work, we target vibrational signatures that are stationary across the sampling period, but short enough to require persistent ("always-on") sensing, while possibly containing spurious mechanical shocks. Previous work has addressed low-power persistent sensing, but not mechanical shocks. Reference [2] introduced a wakeup system at a fixed frequency, with excellent selectivity and 5.4 nW power consumption. Fig. 1(a) shows a simplified circuit diagram of [2]. In [3] (circuit shown in Fig. 1(b)), self-latching replaces the separate latch to further reduce power (5.25 nW for *two* channels). A side effect is integration of the input signal (due to parasitic capacitance), but this integration does not introduce significant shock rejection. This is because the weak feedback limits the input dynamic range such that strongly negative signals can override the latch.

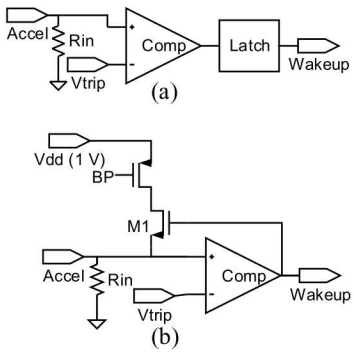

Fig. 1. Simplified schematics for (a) the wakeup circuit in [2] with separate comparator and latch, and (b) the wakeup circuit in [3] with self-latched comparator (single channel shown). The capacitance at the input node performs integration while the feedback through M1 limits the dynamic range.

In addition to resisting mechanical shocks, the system described in this paper can weight (scale) the input amplitudes as part of a support vector machine (SVM) classifier. The benefit of scaling the inputs is that, with multiple channels, the system can be programmed to emphasize, diminish, or even negate different frequencies, thus creating a programmable filter mask. This could improve accuracy and versatility. The system is implemented as up to four MEMS accelerometers coupled to a readout circuit. The circuit performs integration, digitization, and classification leading to the wakeup decision.

This paper is organized as follows. Section II introduces the MEMS device whose model is used as part of the system test. Section III describes the readout circuit. Section IV presents measurements and discusses the results. Section V concludes this paper.

II. Resonant MEMS Accelerometer Model

In this work, we repurpose the microphones from [4] as resonant accelerometers (and will henceforth be referred to as

This work was supported by the DARPA NZERO program managed by Dr. Ronald Polcawich. The views, opinions, and/or findings expressed are those of the author(s) and should not be interpreted as representing the official views or policies of the Department of Defense or the U.S. Government.
<DISTAR and SAND report number here when approved.>

"accelerometers"). In this section we describe the lumped-element model (LEM) for the accelerometers.

The accelerometers consist of a cylindrical diaphragm suspended by folded tethers such that the diaphragm moves out of plane, shown in Fig. 2. The tethers contain aluminum nitride for piezoelectric transduction. The electrodes are arranged to cancel out vibrational modes involving tilting of the mass. Thus, the LEM models a single resonance. This resonance filters the input to selectively amplify (Q-amplification) the resonant frequency while rejecting other frequencies, thus forming the building block for frequency filtering in the system.

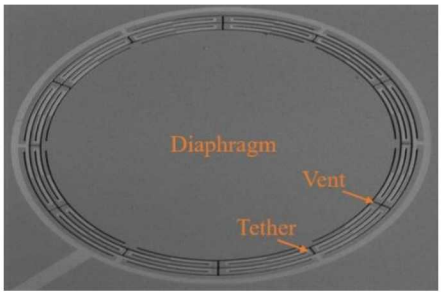

Fig. 2. Microphone from [4] used as an accelerometer in this work.

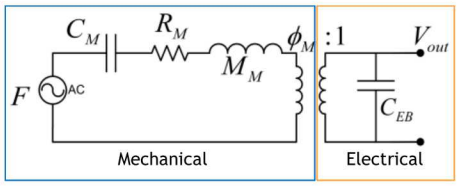

Fig. 3. Lumped-element model of the accelerometer.

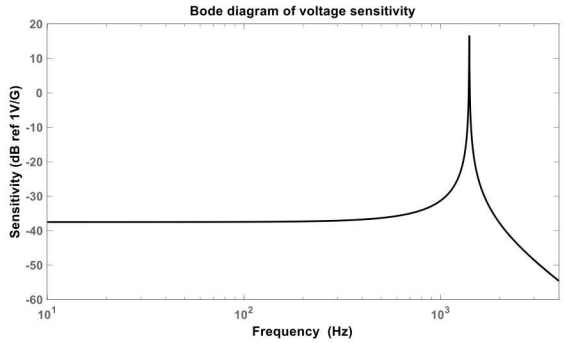

Fig. 4. Frequency response of the accelerometer.

The LEM (Fig. 3, with frequency response in Fig. 4) consists of a mechanical side and electrical side coupled with a transduction factor ϕ_M [5]. The mechanical portion consists of vibrational force F driving a harmonic circuit with C_M (mechanical compliance), R_M (loss), M_M (mass of the diaphragm), and the left side of the ideal transformer. The electrical portion consists of the right side of the transformer and electrical capacitance C_{EB}. The loss R_M is estimated from measurement, while compliance C_M, mass M_M, and capacitance C_{EB} can be calculated from the geometry and material parameters of the device. ϕ_M can be obtained from the effective piezoelectric coefficient and the acoustic compliance when the V_{out} is short-circuited [5]. The resonance frequency of the accelerometer is $f_{res} = \left(2\pi\sqrt{M_M C_M}\right)^{-1}$. The frequency response of an accelerometer is shown Fig. 4 for a 1400 Hz accelerometer with Q assumed (conservatively) to be 500; this is the transfer function used to produce the input voltage data for the measurements in Section IV.

III. CMOS Readout ASIC

The diagram for the readout circuit is shown in Fig. 5:

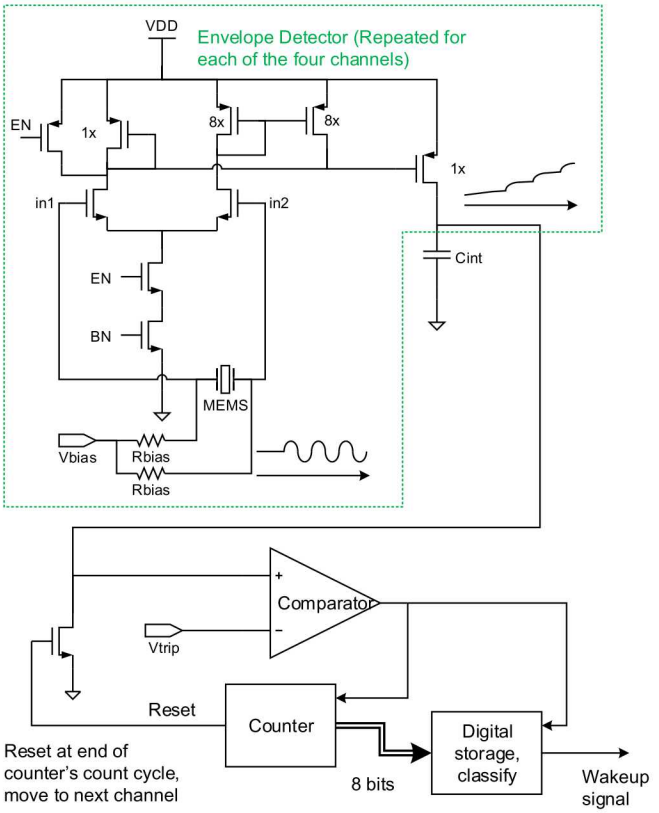

Fig. 5. Schematic for the readout circuit.

The readout ASIC implements the SVM classifier introduced in [6]. The SVM equation implemented is

$$\sum_{ch0}^{ch3} w_k * x_k + bias \overset{?}{\gtrless} 0, \tag{1}$$

where x_k are the individual amplitudes of the sensor channels, w_k are weights for each channel, and *bias* is used to shift the threshold for wakeup. If the sum in (1) is greater than zero, then the circuit produces a wakeup signal.

The circuit employs a single-slope analog-to-digital converter (ADC) to convert the four differential MEMS amplitudes (Ch0 to Ch3) to digital amplitudes x_k. At the input to the ADC, four rectifier-integrator circuits (inside the green dashed line) take turns to sequentially convert amplitude to integration slope. The rectification (envelope detection) occurs because of the asymmetric loads in differential pair causing pinch-off of the output transistor for half the cycle of the input. The integration occurs because the capacitor C_{int} integrates the current at the output of the envelope detector. This integration is

a primary method of shock resistance. Another means of shock resistance is the filtering of the input between the MEMS device capacitance and the R_{bias} resistors.

A comparator (from [2]) compares each slope to user-supplied threshold V_{trip}. When the comparator trips, the count from a 1-2 nW counter is recorded. This count corresponds to the amplitude of the signal; its range of counts is 255 to zero, thus conferring up to eight bits of resolution.

When all four amplitudes have been recorded into the digital storage, the digital cell multiplies (scales) the digitized amplitudes with user-supplied coefficients and executes the classification decision. The choice of frequencies and weights should be informed from the machine-learning upon the data [6], while the bias and V_{trip} may be chosen to also account for mechanical shocks.

IV. Measurements

The circuit is characterized by playing an electronic signal at the input through a 10 pF capacitor (the approximate Thevenin equivalent capacitance of the accelerometers) and measuring the voltage across C_{int} as well as the wakeup signal at the output. The input signal consists of recordings of real-life vibrational data that has been filtered through the MEMS LEM. The use of an electronic signal allows for the introduction of large mechanical shocks into the data while constrained to data from machinery that is difficult to shock.

Fig. 6 shows the Bode diagram segments of frequencies of interest of acceleration data collected from a rotating machine during normal operation (blue trace) and after onset of conditions (vibrations) that, if unchecked, could lead to machine failure (red trace). The amplitude at 1400 Hz (Fig. 6a) increases by about 6 dB upon onset, so we select it as a frequency of interest. Fig. 6b shows the amplitude at 2400Hz, which is used in this paper as an example of a frequency whose amplitude *decreases* upon onset – something that a negative weight can help detect.

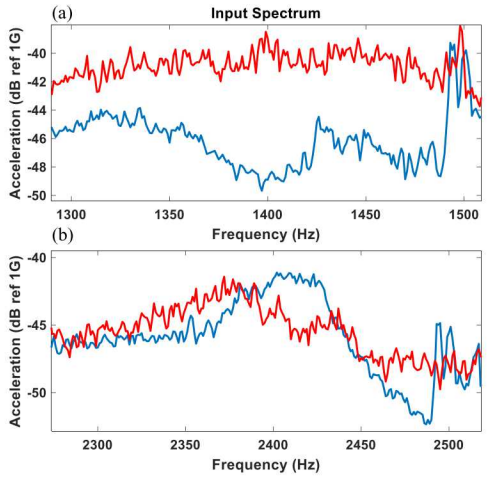

Fig. 6. Bode diagram segments of acceleration data from a rotating machine. Blue: before onset of pre-failure conditions; red: after onset. (a) 1400 Hz frequency whose increase in amplitude indicates onset. (b) 2400 Hz frequency whose decrease in amplitude is associated with onset.

Fig. 7 shows the time series of the acceleration when filtered by the LEM of the MEMS accelerometer at 1400 Hz, with the zoom outset illustrating the ability of the MEMS to filter out all but its resonant frequency. This time series is what is presented to the circuit input Ch2 during measurement.

Fig. 8 shows the time series of the same acceleration filtered by the 2400 Hz LEM. The amplitude is higher before onset than after, so in the SVM we apply a negative weight. This is coupled into the Ch0 input of the circuit.

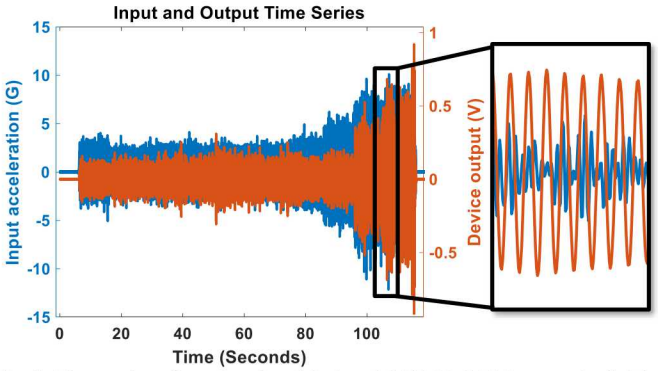

Fig. 7. Time series of acceleration (blue) and 1400 Hz LEM output (red). The outset illustrates the frequency selection of the LEM. The onset of pre-failure conditions occurs at approximately 95 s.

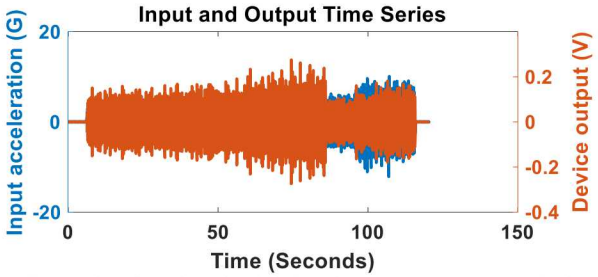

Fig. 8. Time series of acceleration (blue) and 2400 Hz LEM output (red). The amplitude of 2400 Hz decreases after onset.

The circuit output (wakeup signal) and voltage at C_{int} are shown in Fig. 9. The 1400 Hz LEM output is applied Ch2, the 2400 Hz is applied to Ch0, and the other two channels are left at V_{bias}. The sawtooth pattern is from the cycling of the integration slopes of the four channels. The slope that occurs on every fourth channel (Ch3) is due to mismatch in the circuit. The SVM is programmed to have a positive weight for Ch2, negative weight for Ch0, and zero weight for the other channels, and a negative bias that creates the threshold resulting in wakeup only after onset of conditions. The power consumption measured was 4.9 nW. (In order to account for the generation of V_{bias} and V_{trip}, 1.5 nW should be added to the total to power 0.75 nA each across two bias-generation resistors using current mirrors, as in [2]).

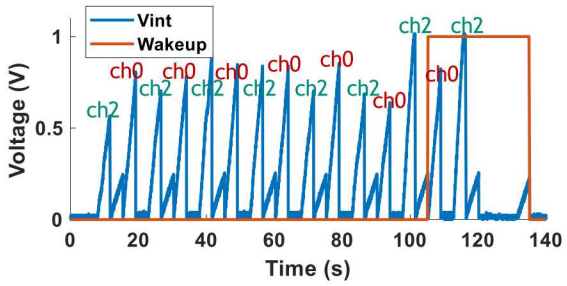

Fig. 9. Circuit output wakeup signal (red) and voltage at Cint (blue), in response to the 1400 Hz and 2400 Hz accelerometer outputs.

To emulate mechanical shock, we add a rectangular pulse of varying magnitude and duration into the vibrational data time series in the pre-onset segment. Fig. 10 shows the time series of a -20 G, 2 s pulse (blue) as filtered through the accelerometer LEM (red). The primary effects on the LEM output are the exponential decay envelope ring-down immediately after the shock, and the DC offset for the duration of the pulse. The offset in voltage output is due to the LEM output being an open-circuit voltage. The R_{bias}, coupled with the device capacitance of about 10 pF, work together to remove this offset when processed by the circuit.

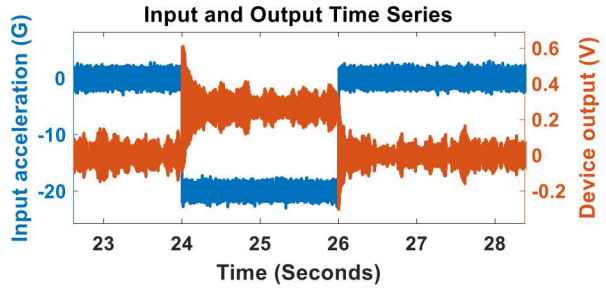

Fig. 10. Mechanical pulse of -20 G, 2s duration applied to the vibrational data (blue), with effect on LEM output shown in red.

The circuit output and voltage at C_{int} in response to the shocked system are shown in Fig. 11. In this experiment, only Ch2 (1400 Hz LEM output) is connected. The circuit does not wake up in response to the shock, while still waking up at the end of the time series due to the condition onset. A detail of the ramp on which the shock is applied is shown in Fig. 12. The shock is applied at 24 s, and the integration slope increases for the duration of the shock. Because of the duration of the integration, the shock does not cause the amplitude to increase appreciably over the baseline (no shock, yellow) amplitude.

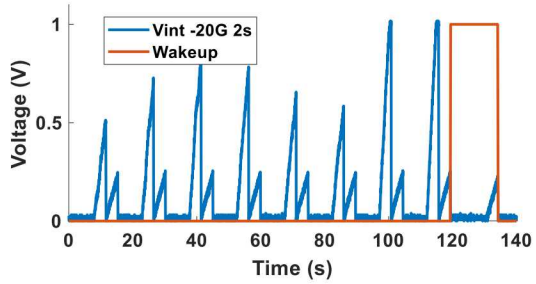

Fig. 11. Circuit output wakeup signal (red) and voltage at Cint (blue), -20 G mechanical shock applied for 2 s at the 24 s mark.

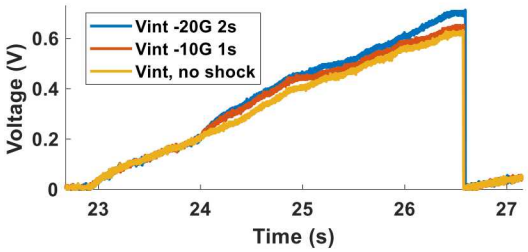

Fig. 12. Detail of the effect of mechanical shock upon the integration slope. The shock is applied at 24 s.

V. Conclusion

We have demonstrated a <10 nW readout circuit capable of rectifying-integrating up to four MEMS accelerometer outputs and performing a wakeup decision using SVM classification. The integration as well as biasing scheme of the devices confer resistance to false positives due to mechanical shock, with measurements showing rejection of a -20 G 2 s shock. This capability along with the SVM implementation make the wakeup system more practical for unattended sensing applications.

Acknowledgment

We thank Kurt Wessendorf for the topology of the envelope detector circuit. Sandia National Laboratories is a multimission laboratory managed and operated by National Technology & Engineering Solutions of Sandia, LLC, a wholly owned subsidiary of Honeywell International Inc., for the U.S. Department of Energy's National Nuclear Security Administration under contract DE-NA0003525.

References

[1] R. H. Olsson, R. B. Bogoslovov and C. Gordon, "Event driven persistent sensing: Overcoming the energy and lifetime limitations in unattended wireless sensors," *2016 IEEE SENSORS*, Orlando, FL, 2016, pp. 1-3.

[2] R. W. Reger *et al*., "Near-zero power accelerometer wakeup system," *2017 IEEE SENSORS*, Glasgow, 2017, pp. 1-3.

[3] R. W. Reger *et al*., "Two-channel wakeup system employing aluminum nitride based MEMS resonant accelerometers for near-zero power applications," *2018 Solid-State Sensors, Actuators, and Microsystems Workshop,* Hilton Head, 2018.

[4] R. W. Reger, P. J. Clews, G. M. Bryan, C. A. Keane, M. D. Henry and B. A. Griffin, "Aluminum nitride piezoelectric microphones as zero-power passive acoustic filters," *2017 19th International Conference on Solid-State Sensors, Actuators and Microsystems (TRANSDUCERS)*, Kaohsiung, 2017, pp. 2207-2210.

[5] S. Horowitz, T. Nishida, L. Cattafesta, and M. Sheplak, "Development of a micromachined piezoelectric microphone for aeroacoustics applications," *Journal of the Acoustical Society of America*, 122:6, pp.3428-3436, 2007.

[6] E. A. Donahue, R. W. Reger, S. Yen, and B. A. Griffin, "On the use of support vector machines for hardware-implementable wakeup system identification," GOMACTech, 2018.